European Journal of Pharmaceutics and Biopharmaceutics 70 (2008) 749–757

Contents lists available at ScienceDirect

European Journal of Pharmaceutics and Biopharmaceutics

journal homepage: www.elsevier.com/locate/ejpb

Research paper

PEGylated chitosan-based polymer micelle as an intracellular delivery carrier for anti-tumor targeting therapy

Fu-Qiang Hu [a,*], Pan Meng [a], You-Qin Dai [b], Yong-Zhong Du [a], Jian You [a], Xiao-Hong Wei [a], Hong Yuan [a]

[a] College of Pharmaceutical Science, Zhejiang University, Hangzhou, PR China
[b] Ningbo No. 2 Hospital, Ningbo, PR China

ARTICLE INFO

Article history:
Received 10 January 2008
Accepted in revised form 16 June 2008
Available online 24 June 2008

Keywords:
Chitosan oligosaccharide
Micelle
Polyethylene glycol
Cellular uptake
Macrophage
In vitro anti-tumor activity

ABSTRACT

Stearic acid-grafted chitosan oligosaccharide (CSO-SA) micelles presented a potential candidate for intracellular drug delivery carrier due to its special spatial structure. In this article, CSO-SA was further modified by polyethylene glycol (PEG). The physicochemical properties of PEGylated CSO-SA (PEG-CSO-SA) micelles were characterized. After PEGylation, the critical micelle concentration (CMC) of PEG-CSO-SA had no significant change; the micelle size increased; and the zeta potential decreased. The cellular uptake of CSO-SA micelles before and after PEGylation in macrophage RAW264.7, immortalized rat liver cells BRL-3A and human liver tumor cells HepG2 was studied. About 58.4 ± 0.63% of CSO-SA micelles were uptaked by RAW264.7 in 24 h, however, only 17.7 ± 0.94% of PEG-CSO-SA micelles were internalized into RAW264.7 after the CSO-SA was modified with PEG in five molar times. Meanwhile, there were no changes in the uptake after PEGylation of CSO-SA in BRL-3A and HepG2. Using mitomycin C as a model drug, the *in vitro* anti-tumor activities of the drug loaded in the micelles were investigated. The 50% cellular growth inhibition (IC_{50}) of the drug decreased from 1.97 ± 0.2 to 0.13 ± 0.02 μg/mL after mitomycin C was loaded into CSO-SA micelles, and the IC_{50} value of the drug had no obvious change when the CSO-SA was modified by PEG.

1. Introduction

The selective controlling of drug concentration and distribution within the tumor microenvironment is one of the most important factors to achieve effective and safe cancer chemotherapy [1–3]. Controlled drug delivery systems using macromolecular conjugates indicated advantages of improving the bio-distribution for existing anticancer drugs, prolonged circulation in the blood stream and tumor-specific accumulation [1,4,5]. Polymeric micelles formed by self-assembly of amphiphilic graft or block copolymers exerted many merits, such as biocompatibility, high drug-loading content, and markedly improved bio-distribution [6–8]. Recently, it was recognized as one of the most promising formulations for anti-tumor drug deliveries, which successfully increased the solubility of many poorly water-soluble drugs [9–11]. It is well known that polymeric micelles have unique core-shell architecture composed of hydrophobic segments as internal core and hydrophilic segments as surrounding corona in aqueous medium. Poorly water-soluble drugs can be solubilized within the hydrophobic core of the micelle. As a result, polymeric micelles can substantially improve the solubility and bioavailability of various hydrophobic drugs [11]. Additionally, the nano-scaled polymeric micelles exhibit tumor localization by enhanced permeability and retention (EPR) effect.

The rapid uptake of many drug carriers by macrophage is still a challenge for clinical application, which may lead to the short half-time of the carrier in blood. A number of strategies are used to overcome the uptake of polymer micelles by macrophage. Among these measures, PEGylation is one of the most popular methods. PEG is a nontoxic and nonirritant hydrophilic polymer [12]. PEGylation of proteins, drugs, liposomes, and nanoparticles has been proven to be an effective approach for extending circulation in the blood stream, owing to the steric hindrance of the PEG chains [13–19]. Similarly, PEGylated polymers may improve the stability of the drug delivery system in the blood by preventing protein absorption and uptake reticuloendothelial systems (RES) [20–22].

Chitosan is a biodegradable, biocompatible cationic polymer with low toxicity. Stearic acid-grafted chitosan oligosaccharide (CSO-SA), which was synthesized by 1-ethyl-3-(3-dimethylaminopropyl)carbodiimide (EDC)-mediated coupling reaction, was demonstrated to form micelle-like structure by self-aggregation in aqueous environment. The hydrophobic cores of the micelles could envelop poorly water-soluble drug, and the drug release could be highly controlled by the shell cross-linking of the micelles [23]. Utilizing the positive charge of the micelles, the plasmid DNA

* Corresponding author. College of Pharmaceutical Science, Zhejiang University, 388 Yuhangtang Road, Hangzhou 310058, PR China. Tel.: +86 571 88208441; fax: +86 571 88208439.
E-mail address: hufq@zju.edu.cn (F.-Q. Hu).

0939-6411/$ - see front matter © 2008 Elsevier B.V. All rights reserved.
doi:10.1016/j.ejpb.2008.06.015

was condensed to prepare gene delivery system, and high gene transfection efficiency was achieved [24]. The CSO-SA micelles could be rapidly internalized into cancer cells due to their cationic property and special spatial structure with multi hydrophobic cores [25]. The results of *in vitro* anti-tumor tests indicated that the IC_{50} value of the drug could be reduced significantly after the drug was loaded into CSO-SA micelles [25,26], and the CSO-SA micelle system could modulate the drug resistance of the cancer cells [26].

The PEGylated CSO-SA with different modification ratio was synthesized here, and the physicochemical properties, such as CMC, micelle size, zeta potential of PEG-CSO-SA, and number of hydrophobic micro-domains per PEG-CSO-SA chain, were investigated in detail. The cellular uptake differences of CSO-SA micelles and PEG-CSO-SA micelles in macrophage, normal cells and tumor cells were compared, using mouse macrophage RAW264.7, immortalized rat liver cells BRL-3A and human liver tumor cells HepG2 as model cells. Mitomycin C was then chosen as a model anti-tumor drug to investigate the drug entrapment efficiency, *in vitro* drug-release profile and *in vitro* anti-tumor activities of drug-loaded CSO-SA micelles and PEG-CSO-SA micelles.

2. Materials and methods

2.1. Materials

Chitosan (M_w = 450.0 kDa, 95% deacetylated degree) was supplied by Yuhuan Marine Biochemistry Co., Ltd., Zhejiang, China. 1-Ethyl-3-(3-dimethylaminopropyl) carbodiimide (EDC) and 2, 4, 6-trinitro-benzene sulfonic acid (TNBS) were purchased from Sigma Chemical Co., St. Louis, USA. Pyrene was purchased from Aldrich Chemical Co., USA. 1-Dodecylpyridinium chloride (DPC) was purchased from Chemical Industries Co., Ltd., Japan. Stearic acid (SA) was purchased from Chemical Reagent Co., Ltd., Shanghai, China. $MPEG_{2000}$ with aldehyde side group was donated by Chinese Academy of Science. Dimethyl sulfoxide (DMSO) was purchased from Haishuo Biochemistry Co., Ltd., Wuxi, China. Mouse macrophage RAW264.7, immortalized rat liver cells BRL-3A and human liver tumor cells HepG2 were purchased from Institute of Biochemistry and Cell Biology, Shanghai, China. Dulbecco's modified Eagle's medium (DMEM) and trypsin–EDTA were purchased from Gibco-BRL, MD, USA. Fetal bovine serum (FBS) was purchased from Sijiqing Biologic Co., Ltd., Zhejiang, China. 3-(4,5-Dimethyl-thiazol-2-yl)- 2,5-diphenyl- tetrazolium bromide (MTT) was purchased from Sigma Chemical Co., St. Louis, USA. Mitomycin C (MMC) was gifted by Zhejiang Hisun Pharmaceutical Co., Ltd., China. All other solvents were of analytical or chromatographic grade.

2.2. Preparation of chitosan oligosaccharide by enzymatic degradation of chitosan [23,24]

A 3% (w/v) chitosan solution was prepared by dispersing 15 g chitosan in 500 mL distilled water. After adding 6.25 mL of 36.5% (w/v) hydrochloric acid, the temperature of the mixture was raised up to 50 °C in a batch reactor, and 1 U/mL chitosanase was added. The reaction time of hydrolysis was controlled by molecular weight measurement of chitosan, which was performed by gel permeation chromatography (GPC). The reaction mixture was then centrifuged for 10 min at 4000 rpm. The supernatant was filtered by a filter with 0.45 μm pole size. The low molecular weight chitosan, chitosan oligosaccharide (CSO), was obtained by lyophilization.

The molecular weight of final chitosan oligosaccharide (CSO) was determined by gel permeation chromatography (GPC) with TSK-gel column (G3000SW, 7.5 mm I.D. × 30 cm) at 25 °C. Master samples of polysaccharide with different molecular weight (M_w = 5.9, 11.8, 22.8, 47.3, 112, 212 kDa) were dissolved in acetate buffer solution (pH 6.0, the mobile phase), and their final concentrations were set to 1.0 mg/mL. Calibration curve was performed by means of polysaccharide samples using the integral molecular weight distribution method. The weighted lyophilized powder of CSO was dissolved in acetate buffer solution (pH 6.0) with a final concentration of 1.0 mg/mL. Ten microliters of the sample was chromatographed with a flow rate of 0.8 mL/min. The molecular weight of CSO was then calculated from the calibration curve.

2.3. Synthesis of CSO-SA and PEG-CSO-SA

The chemical conjugate of CSO-SA was synthesized by the coupling reaction of carboxyl group of stearic acid (SA) with amine group of CSO in the presence of 1-ethyl-3-(3-dimethylaminopropyl) carbodiimide (EDC) [23–26]. Briefly, 500 mg CSO was dissolved in 100 mL de-ionized water (DI water), and 200 mg stearic acid was dissolved in 50 mL hot ethanol, respectively. They were then mixed at 80 °C under mechanic stirring. After 50 mg EDC was added into the mixture, the coupling reaction was carried out for 5 h at 80 °C under mechanic stirring with 250 rpm. After the reaction, the reaction solution was dialyzed against DI water using a dialysis membrane (MWCO: 3.5 kDa, Spectrum Laboratories, Laguna Hills, CA) for 48 h with successive exchange of fresh DI water to remove water-soluble by-products. The reaction solution was then lyophilized. Then the lyophilized powder was further washed with 20 mL ethanol for three times to remove the un-reacted stearic acid. Finally, the product was dispersed in de-ionized water (DI water) and lyophilized.

To obtain PEG-CSO-SA, 200 mg CSO-SA was dissolved in 50 mL DI water. Then $mPEG_{2000}$ with aldehyde side group (the mole ratio of PEG to CSO-SA was varied as 1:5, 1:1, and 5:1) was added into the CSO-SA solution. The solution was stirred overnight at room temperature and then dialyzed against DI water using a dialysis membrane (MWCO: 7 kDa, Spectrum Laboratories, Laguna Hills, CA) for 24 h. The final product was lyophilized. PEG-CSO-SA with different modification ratios was termed as PEG-CSO-SA (1:5), PEG-CSO-SA (1:1), and PEG-CSO-SA (5:1), respectively.

2.4. Characteristics of CSO-SA and PEG-CSO-SA micelles

2.4.1. ^{1}H-NMR analysis

The ^{1}H-NMR spectra of chemicals were obtained by NMR Spectrometer (AC-80, Bruker Biospin, Germany). CSO-SA, PEG, and PEG-CSO-SA were dissolved in D_2O with 0.5 wt%.

2.4.2. Critical micelle concentration

The critical micelle concentrations (CMC) of CSO-SA and PEG-CSO-SA were determined by fluorescence measurement using pyrene as a probe [27]. The fluorescence emission spectra of pyrene in different concentrations (1×10^{-3} to 0.25 mg/mL) of CSO-SA or PEG-CSO-SA solution (containing 6×10^{-7} M of pyrene) were measured using fluorometer (F-2500, HITACHI Co., Japan), with the excitation wavelength set at 334 nm. The slits were set at 10 nm (excitation) and 2.5 nm (emission). The intensities of I_1 and I_3 were measured at the wavelengths corresponding to the first and the third vibronic bands, which were 373 and 384 nm, respectively. The ratio of I_1/I_3 is the so-called pyrene 1:3 ratio index [27].

2.4.3. Micelle size and zeta potential

The average hydrodynamic diameters and zeta potentials of the CSO-SA and PEG-CSO-SA micelle solution (1 mg/mL) in phosphate buffer saline (PBS, pH 7.4) were measured by dynamic light scattering using a Zetasizer (3000HS, Malvern Instruments Ltd., UK).

2.4.4. AFM investigation

The surface properties of CSO-SA and PEG-CSO-SA micelles were observed by an atomic force microscopy (SPA 3800N, SEIKO, Japan). Explorer atomic force microscope was a tapping mode, using high resonant frequency (F_0 = 129 kHz), pyramidal cantilevers with silicon probes having force constants of 20 N/m. Scan speed was set at 2 Hz. The samples were dissolved in PBS (pH 7.4) and then dropped on freshly cleaved mica plates, followed by vacuum-drying for 24 h at 25 °C.

2.4.5. Degree of amino-substitution

The degrees of amino-substitution for CSO-SA and PEG-CSO-SA were assayed using TNBS reaction [23,24,28–30]. Two milliliters of CSO-SA or PEG-CSO-SA solution (containing 300 μg CSO-SA or PEG-CSO-SA), 2 mL of 4% $NaHCO_3$ (pH 8.5) and 2 mL of 0.1% aqueous TNBS solution were added. The reaction was carried out at 37 °C for 2 h, followed by the addition of 2 mL HCl (2 N). The UV absorbance of the solution was measured at 344 nm by a UV spectrophotometer (TU-1800PC, Beijing, Purkinje General Instrument Co., Ltd., China). Calibration curve was obtained with CSO solution with different concentrations. The degree of substitution termed as the substitute number by SA or PEG per one hundred amino groups in CSO molecules was then calculated from the UV absorbance of CSO-SA (or PEG-CSO-SA) and CSO solution with the same content.

2.4.6. Number of hydrophobic micro-domains per CSO-SA or PEG-CSO-SA molecule

The number of hydrophobic micro-domains per CSO-SA or PEG-CSO-SA molecule in the micelles was estimated by steady-state fluorescence-quenching method [31] using 1-dodecylpyridinium chloride (DPC) as quencher. Briefly, 0, 0.2, 0.4, 0.6, 0.8, and 1.0 mL of DPC ethanol solution (1.0×10^{-4} M) was added into the test tube, respectively. These test tubes were then maintained at 100 °C to remove ethanol. Five milliliters of CSO-SA or PEG-CSO-SA solution (0.4 mg/mL) was added into different test tubes containing pyrene, followed by ultrasonic treatment (Sonic Purger CQ250, Academy of Shanghai Shipping Electric Instrument) in water bath at room temperature for 30 min. The micelle solution containing 6.0×10^{-7} M of pyrene was then added into the test tubes containing different amount of DPC. Fluorescence spectra were recorded by a fluorometer (F-2500, HITACHI Co., Japan) at room temperature. The excitation wavelength, emission wavelength and slit were set at 337, 393, and 5 nm, respectively.

2.5. Cell culture

Mouse macrophage RAW264.7, human liver tumor cells HepG2 and immortalized rat liver cells BRL-3A were maintained in DMEM supplemented with 10% (v/v) FBS (fetal bovine serum) and penicillin/streptomycin (100 U/mL) at 37 °C and 5% CO_2. Cells were subcultured regularly using trypsin/EDTA.

2.6. Cellular uptake

2.6.1. Preparation of FITC-labeled CSO-SA and PEG-CSO-SA micelles

FITC-labeled CSO-SA or PEG-CSO-SA micelles were prepared by adding FITC ethanol solution into 5.0 mg/mL CSO-SA or PEG-CSO-SA aqueous solution. The molar ratio of CSO-SA (or PEG-CSO-SA) to FITC was set at 1:4. The reaction solutions were stirred overnight with 250 rpm at room temperature under protection from light, followed by their being dialyzed against DI water using a dialysis membrane (MWCO: 3.5 kDa, Spectrum Laboratories, Laguna Hills, CA) for 6 h to remove the un-reacted FITC. Then, the dialyzed product was lyophilized to receive FITC-labeled CSO-SA and PEG-CSO-SA.

2.6.2. Quantification of cellular uptake

RAW264.7, HepG2, and BRL-3A cells were seeded at 1.0×10^5/mL cells per well in a 24-well plate (Nalge Nunc International, Naperville, IL, USA) and allowed to attach for 24 h, respectively. After removing the growth medium, one milliliter DMEM containing 100 μg FITC-labeled CSO-SA or PEG-CSO-SA was added into each well, followed by further incubation for 1.5, 3, 6, 12, and 24 h, respectively. After the cells were washed with PBS for three times, 50 μL of trypsin PBS solution (2.5 mg/mL) was added into each well. After the further incubation for 15 min, 1 mL PBS was added into each well, and the cells were harvested. The harvested cells were fragmented through ultrasonic treatment. Finally, the cell lysate was subjected to fluorescence assay using fluorometer (F-2500, HITACHI Co., Japan) (excitation wavelength: 495 nm; emission wavelength: 521 nm). The cellular uptake contents of CSO-SA or PEG-CSO-SA micelles were corrected to per microgram intracellular protein. Using BCA protein assay kit, the intracellular protein content was measured. Briefly, 20 μL cell lysate was added into each well, and 200 μL BCA working reagent was then added, followed by incubation at 37 °C for 30 min. UV absorbance at 570 nm of cell lysate was measured by a microplate reader (Bio-Rad, Model 680, USA). The protein concentration was calculated from calibration curve obtained from bovine serum albumin (BSA). The cellular uptake percentage of micelles was calculated from the following equation:

$$P_t\ (\%) = F_t/F_0 \times 100\%, \quad (1)$$

where P_t represents the cellular uptake percentage of the micelles at t time; F_t and F_0 are the fluorescence absorbance corrected by intracellular protein concentration at t time and 0 time, respectively.

2.7. Preparation of MMC-loaded CSO-SA and PEG-CSO-SA micelle

Desired volume of mitomycin C (MMC) PBS (pH 7.4) solution was added into CSO-SA or PEG-CSO-SA/PBS (pH 7.4) solution (whose final concentration is 5 mg/mL) The mixture was subjected to probe-type ultrasonic treatment (400 W, 20 cycles with 2 s active-3 s duration, JY92-II, Scientz Biotechnology Co., Ltd., China) to obtain MMC-loaded micelles with a different MMC concentration. The MMC-loaded CSO-SA micelles were termed as CSO-SA/MMC, and MMC-loaded PEG-CSO-SA micelles with different PEG modification ratio were termed as PEG-CSO-SA (1:5)/MMC, PEG-CSO-SA (1:1)/MMC, and PEG-CSO-SA (5:1)/MMC, respectively.

The drug entrapment efficiency (EE) of the MMC-loaded micelles was measured by HPLC method using an AgilentG1310A pump (1100 Series) unit control, an Agilent G1314AVariableWavelength Detector (1100 Series) set at 365 nm. A Dikma Diamonsil C18 column (250 mm × 4.6 mm, 5 μm) was used. The mobile phase consisted of methanol and sodium acetate–acetic acid buffer solution (30:70, v/v). The column temperature was set at 25 °C. The calibration curve of the peak area against MMC concentration was $y = 66.605x - 65.425$, with the MMC concentration varying from 0.5 to 100 μg/mL (R^2 = 0.9996, where y = peak area and x = concentration of MMC).

Four hundred microliters of MMC-loaded micelles were added into ultrafilter (MWCO: 3.0 kDa, Millipore, Carrigtwohill, Co., Cork, Ireland), and the tube was centrifuged under 10,000 rpm for 10 min. The MMC content in the ultrafiltrate was regarded as unentrapped drug (Mu) which was measured by HPLC method. For determination of the total MMC content (M) in the micelle solution, 800 μL of DMSO was added into 400 μL of MMC-loaded micelles, followed by ultrasonic treatment (Sonic Purger CQ250, Academy of Shanghai Shipping Electric Instrument) in water bath at room temperature for 15 min. After being filtered with 0.22 μm millipore filter, the MMC content was determined by

HPLC method. The EE of MMC-loaded micelles was calculated as described below:

$$\text{EE}\ (\%) = (M - \text{Mu})/M \times 100\%, \quad (2)$$

where M represents the total MMC content in the micelle solution, and Mu is the MMC content in the ultrafiltrate.

2.8. In vitro MMC release from the micelles

One milliliter of MMC-loaded CSO-SA micelle solution or MMC-loaded PEG-CSO-SA micelle solution was added into a dialysis tube (MWCO: 7 kDa, Spectrum Laboratories, Laguna Hills, CA) and then placed in a plastic tube containing 20 mL of PBS (pH 7.4) solution. The tests were conducted in incubator shaker (HZ-8812S, Scientific and Educational Equipment plant, Tai Cang, China), which was maintained at 37 °C and shaken horizontally at 60 rpm. One milliliter sample was withdrawn from the system at defined time and filtered with 0.22 μm millipore filter. The drug concentration in the filtrate was determined by HPLC method as described above. The diffusion of MMC solution from the dialysis tube was conducted as control.

2.9. Cytotoxicity assay

HepG2 cells were seeded in a 96-well plate at a seeding density of 10,000 cells per well in 0.2 mL of growth medium consisting of DMEM with 10% FBS and antibiotics. After the cells were cultured at 37 °C for 24 h, the growth medium was removed and fresh growth medium containing the desired amounts of blank micelles, free MMC and MMC-loaded CSO-SA or PEG-CSO-SA micelles was added. The cells were further incubated for 48 h. After the incubation, 60 μL of 5 mg/mL MTT was added to each well, and cells were incubated for another 4 h. Each well was then washed with 100 μL of PBS after the medium containing un-reacted MTT was removed, and 180 μL of DMSO was then added to each well to dissolve the MTT formazan crystals. After the plates were shaken for 20 min, the absorbance of formazan product was measured at 570 nm in a microplate reader (Bio-Rad, Model 680, USA). Survival percentages of each well were calculated taking the mock-treated cells as 100% [32].

2.10. Determination of intercellular mitomycin C concentration

HepG2 cells were seeded in a 24-well plate(Nalge Nunc International, Naperville, IL, USA) at a seeding density of 1.0×10^5/mL cells per well and allowed to attach for 24 h. Cells were then incubated with MMC PBS solution and MMC-loaded CSO-SA or PEG-CSO-SA micelle solution (drug concentration: 5 μg/mL) in growth medium for 3, 6, 8, 10, and 12 h. The cells were then washed with PBS thrice, and 50 μL trypsin PBS solution (2.5 mg/mL) was added. After the cells were further incubated for 15 min, the cells were harvested by adding 450 μL de-ionized water, and were then subjected to probe-type ultrasonic treatment (400 W, 10 cycles with 2 s active-3 s duration, JY92-II, Scientz Biotechnology Co., Ltd., China) in ice bath. The obtained cell lysate was diluted with the same volume of mobile phase of HPLC and then filtered with 0.22 μm millipore filter. The MMC concentration in the filtrate was determined by HPLC method. The protein content in the cell lysate was measured using the Micro BCA protein assay kit. The uptake percentages of the drug were calculated from Eq. (3).

$$\text{Drug-uptake percentage}\ (\%) = C_t/C_0 \times 100\%, \quad (3)$$

where C_t and C_0 are the intracellular MMC concentration corrected by intracellular protein concentration at t time and 0 time, respectively.

3. Results and discussion

3.1. Synthesis of CSO-SA and PEG-CSO-SA

The CSO with 28 kDa of weight average molecular weight was used to synthesize the CSO-SA. CSO-SA was synthesized by the coupling reaction between the amino groups of CSO and carboxyl groups of SA in the presence of water-soluble EDC, and the PEGylation of CSO-SA was conducted by the reaction of the remaining amino groups of CSO-SA and aldehyde groups of PEG. ^{1}H-NMR spectra of CSO-SA and PEG-CSO-SA are shown in Fig. 1. As reported in the previous research [23,25], the chemical shift of the proton for stearate groups appeared near 1 ppm. Compared with CSO-SA, the ^{1}H-NMR spectrum of the PEG-CSO-SA (5:1) (Fig. 3B) showed a sharp signal at δ = 3.5–3.65 ppm, which was the chemical shifts of the proton of $-CH_2CH_2O-$ for PEG. It was also confirmed that the proton of aldehyde groups (δ = 9.6) for PEG disappeared in the ^{1}H-NMR spectrum (data was not shown). These results indicated that PEG was coupled to CSO-SA.

To determine the graft ratio of SA and PEG, the degrees of amino-substitution (DS) of CSO-SA and PEG-CSO-SA were measured using TNBS method. The results are shown in Table 1. The DS of CSO-SA was about 8.8 ± 0.2%, and the DS of PEG-CSO-SA increased with increasing the charge ratio of PEG. The results also confirmed the graft reaction of SA to CSO and the PEGylation of CSO-SA. The DS value of PEG-CSO-SA higher than the theoretical value might cause the test error originating from the barrier shield effect of PEG chain.

3.2. Characteristics of CSO-SA and PEG-CSO-SA micelles

CSO-SA micelles were easily obtained by dispersing CSO-SA into aqueous solution. After the PEGylation, PEG-CSO-SA micelles also formed readily. The number of average size and zeta potential of CSO-SA and PEG-CSO-SA micelles (1 mg/mL in PBS, pH 7.4) are shown in Table 1. The results showed that the size of PEG-CSO-SA micelles increased with increasing the modification ratio of PEG, which resulted from the stretch of PEG chains on the PEG-CSO-SA micelle surface toward water phase. The size distributions of CSO-SA and PEG-CSO-SA micelles are shown in Fig. 2. It was clear that the micelle size-distribution became narrow after the PEGylation of CSO-SA. Because the pH of body fluid is near neutral, the information of physicochemical properties for present micelles in neutral environment is very important. In this study, the zeta

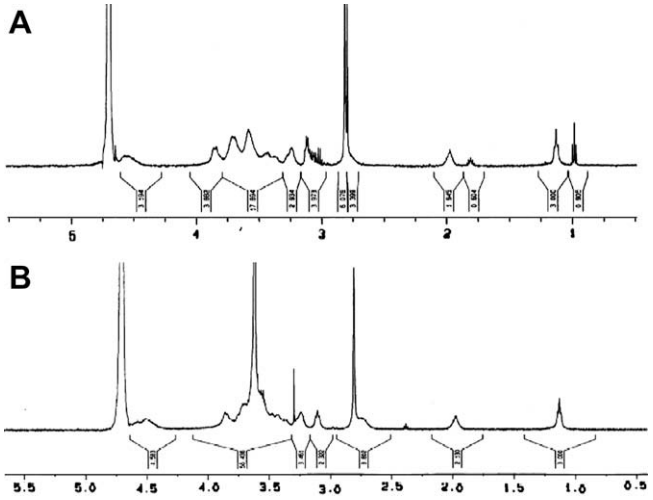

Fig. 1. ^{1}H-NMR spectra of (A) CSO-SA; (B) PEG-CSO-SA (5:1).

Table 1
Characteristics of CSO-SA and PEG-CSO-SA micelles

Formula	Size (nm)	Zeta (mV)	CMC (μg/mL)	DS (%)	n_{SA} (−)	n_{domain} (−)
CSO-SA	103.4 ± 5.1	20.1 ± 1.8	13.8	8.8 ± 0.2	4.5 ± 0.3	3.2 ± 0.2
PEG-CSO-SA (1:5)	119.2 ± 7.5	14.5 ± 5.8	12.5	11.8 ± 1.1	5.4 ± 0.3	2.7 ± 0.2
PEG-CSO-SA (1:1)	161.2 ± 4.8	14.3 ± 4.6	11.5	14.7 ± 1.0	6.8 ± 0.4	2.1 ± 0.1
PEG-CSO-SA (5:1)	171.8 ± 9.2	15.9 ± 5.3	11.7	19.8 ± 0.3	7.8 ± 0.2	1.8 ± 0.1

DS, n_{SA}, and n_{domain} indicate the degree of amino-substitution, the aggregate number of SA groups per hydrophobic micro-domain, and the number of hydrophobic micro-domain per copolymer chain. Data represent the mean ± standard deviation (n = 3).

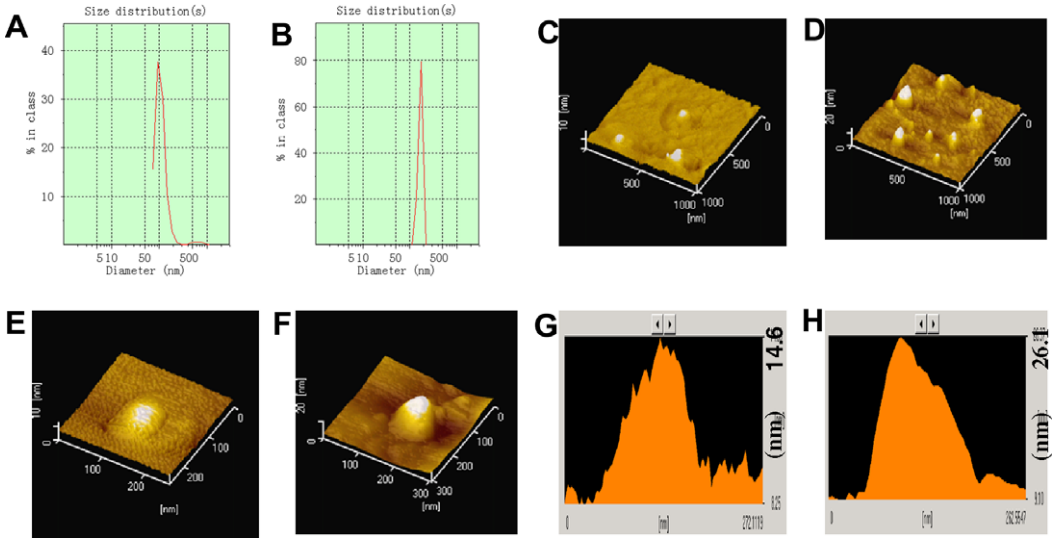

Fig. 2. Size distribution and AFM images of CSO-SA and PEG-CSO-SA (5:1) micelles. (A) Size distribution of CSO-SA micelles; (B) size distribution of PEG-CSO-SA (5:1) micelles; (C) AFM three-dimension images of CSO-SA micelles; (D) AFM three-dimension images of PEG-CSO-SA (5:1) micelles; (E) zoom-in image of one CSO-SA micelle; (F) zoom-in image of one PEG-CSO-SA (5:1) micelle; (G) cross-section images of CSO-SA micelles; (H) cross-section images of PEG-CSO-SA (5:1) micelles.

potential of CSO-SA micelles in pH 7.4 PBS was found to be 20.1 ± 1.8 mV. As reported elsewhere [23–26], the zeta potential of CSO-SA micelles in DI water was above 40 mV. The decrease in zeta potential of CSO-SA micelles resulted from the increased pH value of the medium. The pK_a of the amino group for chitosan is about 5.6. Therefore, the zeta potential in PBS (pH 7.4) decreased, compared with that in DI water. Moreover, the zeta potential of PEG-CSO-SA micelles was a little lower than that of CSO-SA micelles, which might be caused from the barrier shield effect of PEG chain on the micelles [33] and the reduced amino groups after the PEGylation.

AFM technique has been widely applied to obtain surface morphological information of nanoparticles [34]. Fig. 2 also gives the tapping mode AFM images of CSO-SA and PEG-CSO-SA micelles. The observed AFM image of CSO-SA micelles might result from the collapse of micelle during vacuum-drying process [35]. It can be seen from Fig. 2E–H that the collapse of PEG-CSO-SA micelles was not as severe as that of CSO-SA micelles, suggesting that maybe PEGylation can protect the micelle from collapsing during vacuum-drying process to some extent. Furthermore, surface analysis images of CSO-SA and PEG-CSO-SA micelles in Fig. 2E–H showed that the micelle surface was much smoother after the PEGylation. It can be attributed to the insert of PEG chains into the crevice on the micelle surface during the dry process.

The critical micelle concentration (CMC) is an important characteristic for amphiphilic copolymers, indicating the self-aggregation ability of the amphiphilic copolymer. The aggregation behavior of CSO-SA and PEG-CSO-SA in PBS (pH 7.4) was investigated by fluorometry using pyrene as a fluorescent probe [27]. Fig. 3 shows the change in the value of I_1/I_3 against the logarithm of CSO-SA or PEG-CSO-SA concentration. Before the micelle formed in aqueous environment, the value of I_1/I_3 remained almost the same. The higher value of I_1/I_3 after the PEGylation might originate from the effect of PEG on the fluorescence intensity [36]. Once the polymer concentration reached above the CMC, the value of I_1/I_3 deceased sharply, indicating the formation of micelles. The CMC values of

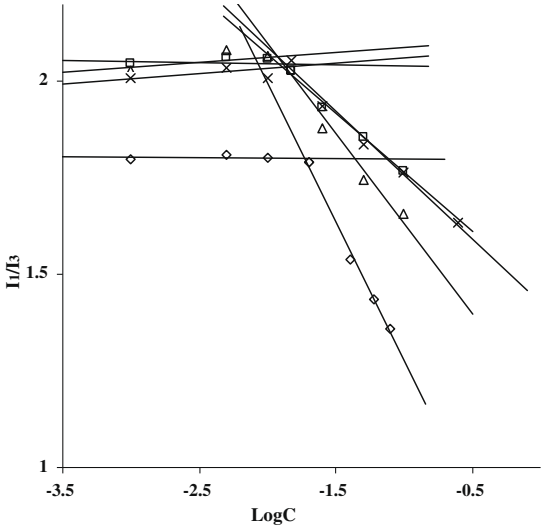

Fig. 3. Plots of I_1/I_3 against the logarithm of CSO-SA or PEG-CSO-SA concentration. (◇): CSO-SA; (□): PEG-CSO-SA (1:5); (×) PEG-CSO-SA (1:1); (□) PEG-CSO-SA (5:1). Data represent the mean ± standard deviation (n = 3).

CSO-SA and PEG-CSO-SA in PBS (pH 7.4) are shown in Table 1. The CMC values varied from 11.7 to 13.8 μg/mL, which were much lower than those of low molecular weight surfactants in water [37]. The CMC values of PEG-CSO-SA were almost the same compared to those of CSO-SA.

In previous researches [25,26], it was reported that the CSO-SA micelle presented rapid cellular uptake, and was a potential candidate for intracellular drug delivery carrier. The rapid cellular uptake of CSO-SA micelles contributed to the positive charge and the special spatial structure. The CSO-SA micelles had multihydrophobic core, which formed the self-aggregation process of CSO-SA due to the special rigidity of chitosan oligosaccharide chain. The hydrophobic core near the micelle surface might facilitate the internalization of the micelles into cells. To investigate the spatial structure of the micelles after the PEGylation, the aggregation number of SA groups per hydrophobic micro-domain (n_{SA}) and the number of hydrophobic micro-domains per copolymer chain (n_{domain}) were estimated by the steady-state fluorescence-quenching method using DPC as a fluorescence quencher [31]. The steady-state quenching data fit in quenching kinetics:

$$\ln(I_0/I) = [Q]/[M], \quad (4)$$

where I_0 and I are the fluorescence emission intensities in the absence and presence of quencher, respectively, [Q] is the concentration of the quencher, and [M] is the concentration of hydrophobic micro-domains in micelle. Thus, the aggregation number of SA groups per hydrophobic micro-domain (n_{SA}) can be calculated by Eq. (5),

$$n_{SA} = [SA]/[M], \quad (5)$$

where [SA] and [M] represent the concentrations of SA and hydrophobic micro-domain, respectively. Therefore, the number of hydrophobic micro-domains per CSO-SA or PEG-CSO-SA molecule (n_{domain}) can be calculated by Eq. (6).

$$n_{domain} = N_{SA}/n_{SA}, \quad (6)$$

where n_{SA} is the number of SA groups in one CSO-SA or PEG-CSO-SA molecules.

Fig. 4 shows the plot of $\ln(I_0/I)$ of pyrene fluorescence against DPC concentration in the presence of 0.4 mg/mL CSO-SA or PEG-CSO-SA. The n_{SA} and n_{domain} of the micelles are shown in Table 1. It was found that the n_{SA} increased and the n_{domain} decreased with increasing the modification ratio of PEG. The results indicated that the introduction of hydrophilic PEG chain into the CSO-SA molecule reduced the number of hydrophobic micro-domains in micelle. However, even for the PEG-CSO-SA with the highest PEG modification ratio, the micelles still kept the special spatial structure with multihydrophobic micro-domains.

3.3. Effect of PEGylation of CSO-SA on the cellular uptake

In general, biocompatibility is an important requirement for the application of colloidal carriers in humans. To avoid recognition by mononuclear phagocyte system (MPS), PEG is the most popular material to modify particulate surfaces. Herein, the cellular uptake of CSO-SA micelles before and after PEGylation was conducted, using mouse macrophage RAW264.7, immortalized rat liver cells BRL-3A and human liver tumor cells HepG2 as model macrophage, normal liver cells and liver tumor cells. Immortalized rat liver cell had been used as normal liver cells to evaluate cellular uptake and cytotoxicity of nanoparticles [38].

The cellular uptake percentages of CSO-SA and PEG-CSO-SA micelles in RAW264.7, HepG2, and BRL-3A are shown in Fig. 5. It was found that the cellular uptake percentages of CSO-SA micelles in normal cells and tumor cells were almost the same, and the PEGylation of CSO-SA did not affect the cellular uptake of the micelles ($p > 0.05$). However, comparing with CSO-SA micelles, the internalization of PEG-CSO-SA micelles into macrophage reduced significantly. About 58.4 ± 0.63% of CSO-SA micelles were uptaked by RAW264.7 in 24 h. Only 17.7 ± 0.94% of PEG-CSO-SA (1:5) micelles were internalized into RAW264.7 in 24 h. The results indicated that PEG modification can significantly reduce the internalization of the CSO-SA micelles into macrophage, while the cellular uptake percentages of PEG-CSO-SA micelles by HepG2 and BRL-3A remained almost the same as those of CSO-SA micelles. Although the number of hydrophobic micro-domains per copolymer chain reduced after the PEGylation of CSO-SA, the introduction of hydrophilic PEG chains on the micelle surface could increase the interaction between cellular membranes and the PEG chain [39]. Because the PEGylation of CSO-SA did not reduce the cellular uptake of the micelles by normal liver cells, a further ligand modification of the micelles was a future challenge to enhance the internalization into tumor cells and to reduce the uptake by normal cells.

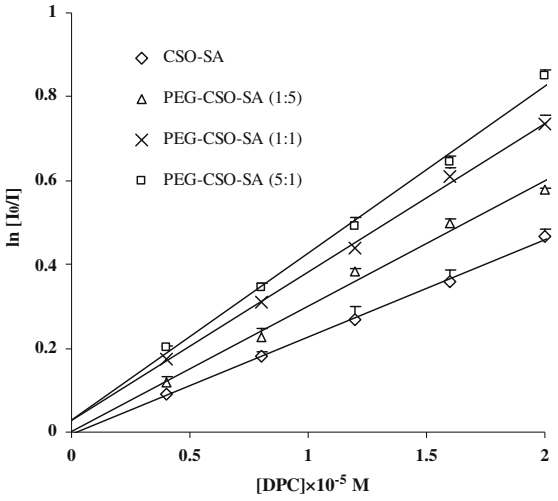

Fig. 4. Plots of ln (I_0/I) of pyrene fluorescence against the DPC concentration in the presence of 0.4 mg/mL CSO-SA or PEG-CSO-SA. Data represent the mean ± standard deviation ($n = 3$).

3.4. In vitro anti-tumor activity

Using MMC as a model anti-tumor drug, *in vitro* anti-tumor activities of MMC-loaded CSO-SA micelles before and after the PEGylation were studied. The MMC-loaded micelle solution used in MTT assay was subjected to the determination of drug entrapment efficacy (EE) using the HPLC method. The peak area had a good linear relation to the concentration of MMC in the range from 0.5 to 100 μg/mL. The results shown in Table 2 indicate that there is no significant difference among the EE of the micelles before and after the PEGylation ($p > 0.05$), suggesting that PEGylation did not affect the drug-entrapment ability of CSO-SA micelles.

In vitro MMC release profiles from CSO-SA and PEG-CSO-SA micelles are shown in Fig. 6. All the formulas show a complete MMC release in 12 h. The fast drug-release from the micelles may be due to the relatively high hydrophilicity of MMC. Moreover, no significant difference was found between MMC-loaded CSO-SA micelles and MMC-loaded PEG-CSO-SA micelles. This result indicates that PEGylation had no effect on the MMC release from the micelles, which might have contributed to the hydrophilicity of MMC and the fast drug-release from CSO-SA micelles.

Table 2 also shows the IC_{50} value of the free drug, blank micelles and MMC-loaded micelles, respectively. Using MTT method, the

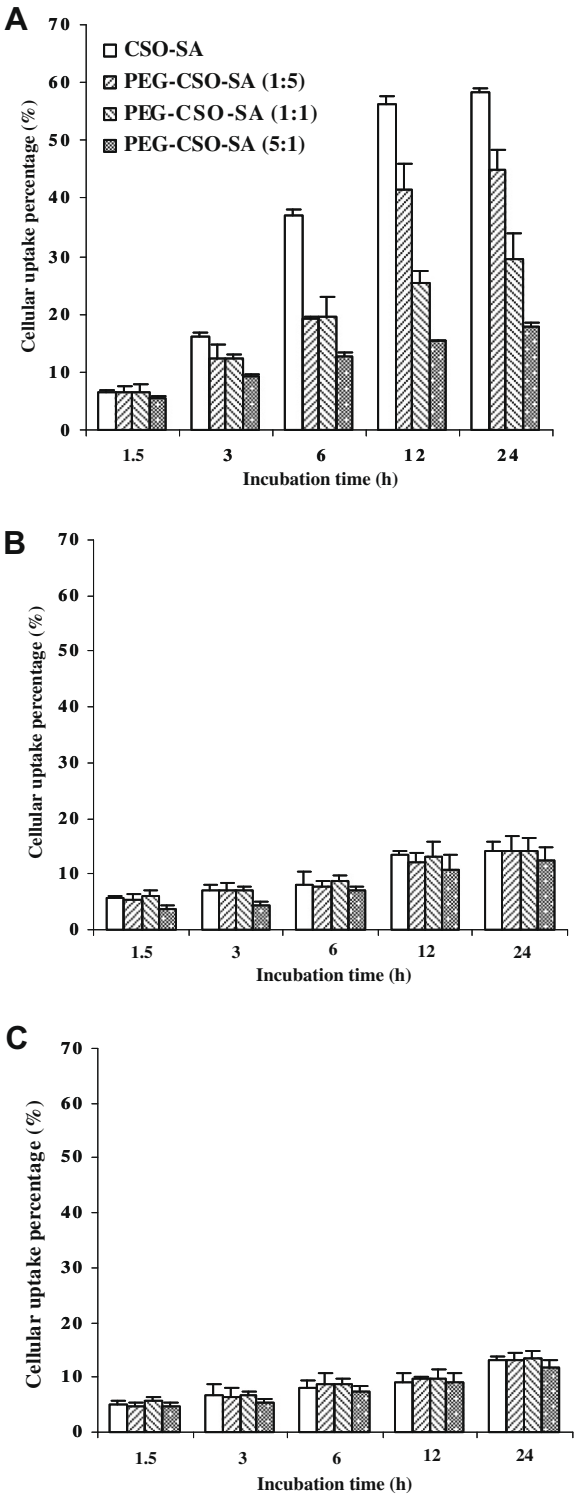

Fig. 5. Cell-uptake percentages of CSO-SA micelles and PEG-CSO-SA micelles in different cell lines. (A) RAW264.7; (B) HepG2; (C) BRL-3A. Data represent the mean ± standard deviation ($n = 4$).

IC_{50} values of CSO-SA and PEG-CSO-SA were first determined as about 400 μg/mL, indicating that the present micelles can be used as a safe drug-carrier. PEG modification of CSO-SA did not increase the cytotoxicity of the micelle ($p > 0.05$). The relationships between cell growth inhibition and the concentration of CSO-SA or PEG-CSO-SA are shown in Fig. 7.

Table 2
IC_{50} and EE of the free MMC, blank micelles, and MMC-loaded micelles

Formula	IC_{50} (μg/mL)	EE (%)
Free MMC	1.97 ± 0.2	–
CSO-SA	392.4 ± 7.3	–
PEG-CSO-SA (1:5)	386.0 ± 14.0	–
PEG-CSO-SA (1:1)	383.6 ± 1.9	–
PEG-CSO-SA (5:1)	390.2 ± 13.4	–
MMC-loaded CSO-SA	0.13 ± 0.02	32.3 ± 2.3
MMC-loaded PEG-CSO-SA (1:5)	0.12 ± 0.03	35.6 ± 1.1
MMC-loaded PEG-CSO-SA (1:1)	0.14 ± 0.04	33.2 ± 1.0
MMC-loaded PEG-CSO-SA (5:1)	0.11 ± 0	37.4 ± 2.3

Data represent the mean ± standard deviation ($n = 3$).

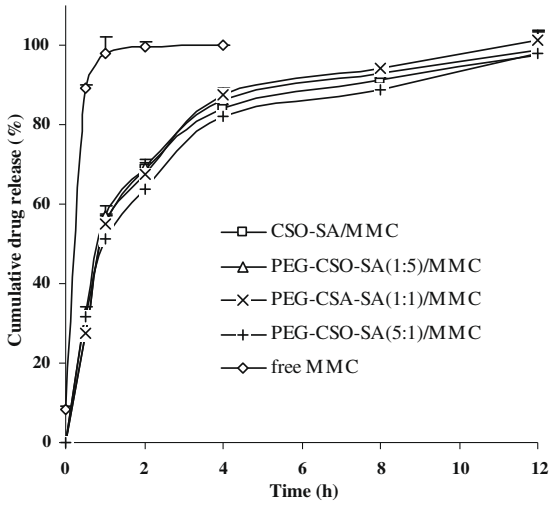

Fig. 6. *In vitro* drug-release profiles from CSO-SA micelles to PEG-CSO-SA micelles. Data represent the mean ± standard deviation ($n = 3$).

Fig. 8 shows the variation of cell growth inhibition against the drug concentration using a different formula. The IC_{50} value of free MMC was about 1.97 ± 0.2 μg/mL. After 32.3 ± 2.3% of the drug was loaded into CSO-SA micelles, the IC_{50} value decreased to 0.13 ± 0.02 μg/mL. This result means that the same *in vitro* anti-tumor activity can be reached when CSO-SA micelles are used as a drug transport carrier, and that the drug dosage is reduced about

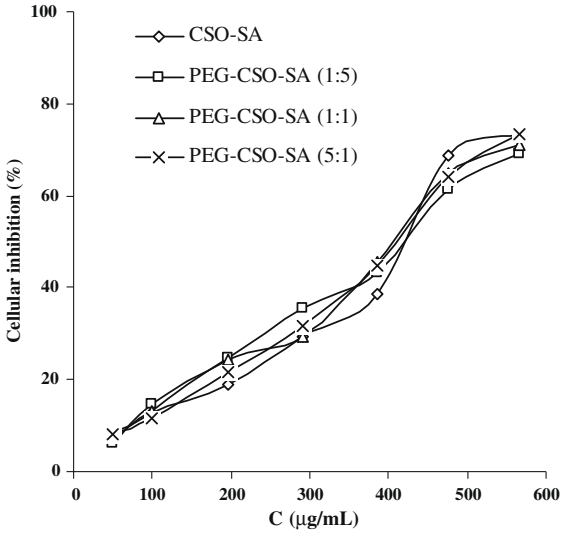

Fig. 7. Variation of the cellular growth inhibition against the concentrations of CSO-SA and PEG-CSO-SA micelles. Data represent the mean ± standard deviation ($n = 3$).

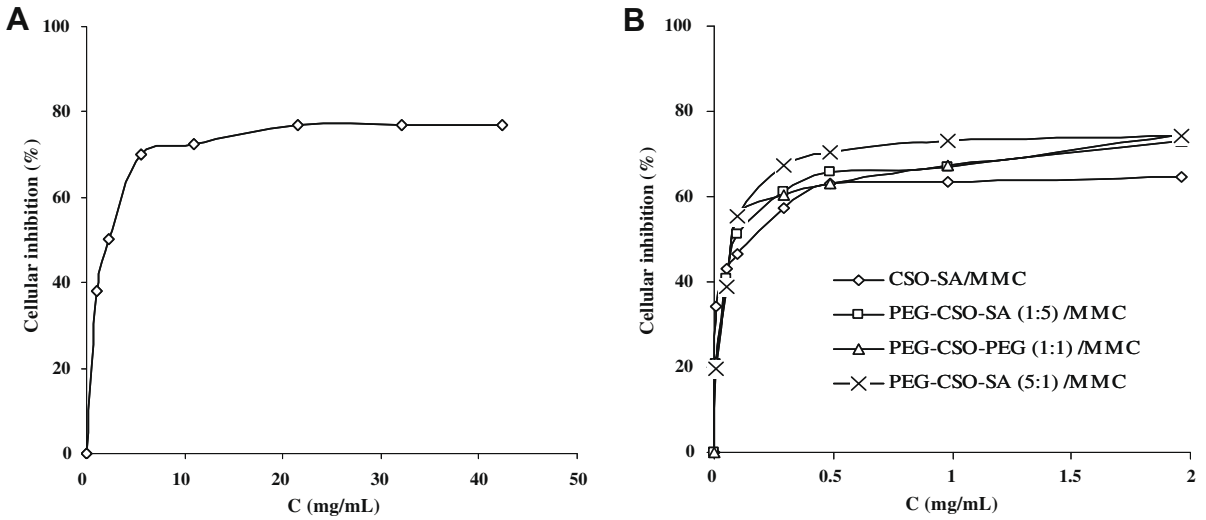

Fig. 8. Variation of the cellular growth inhibition against the drug concentration. (A) free drug; (B) MMC-loaded micelles. (◇): CSO-SA micelles; (□): PEG-CSO-SA (the molar ratio of PEG to CSO-SA was 1:5) micelles; (□) PEG-CSO-SA (the molar ratio of PEG to CSO-SA was 1:1) micelles; (×) PEG-CSO-SA (the molar ratio of PEG to CSO-SA was 5:1)micelles. Data represent the mean ($n = 3$).

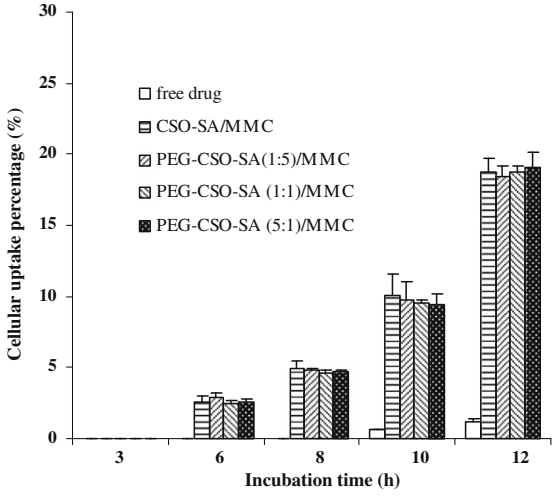

Fig. 9. Intracellular MMC concentrations against the incubation time after the cells were incubated with the free MMC, MMC-loaded CSO-SA micelles and MMC-loaded PEG-CSO-SA micelles. Data represent the mean ($n = 3$).

14 times. The increased cytotoxicity of MMC-loaded CSO-SA micelles could have contributed to the faster cellular uptake of CSO-SA micelle than that of the free drug. Moreover, the IC_{50} value of MMC-loaded PEG-CSO-SA micelles did not change obviously ($p > 0.05$), which might have been due to the similar cellular uptake, drug entrapment efficiency and drug release profile of MMC-loaded micelles.

To clear the relationship between the cytotoxicity and the drug concentration in cells, the determination of intracellular MMC concentrations was done. Fig. 9 shows the cellular uptake percentages of MMC delivered by CSO-SA micelles, PEG-CSO-SA micelles and the MMC solution. Due to the determination limit of HPLC, the drug contents used in cellular uptake were higher than those in cytotoxicity tests, and all the tests were stopped at 12 h because of the high cellular growth inhibition as the incubation time prolonged. It was clear that the CSO-SA micelles could mediate the internalization of MMC into cancer cells, and the intracellular MMC concentration of MMC-loaded CSO-SA micelles was higher than that of the MMC solution. About 18% of the drug was internalized into cancer cells in 12 h when the CSO-SA micelles were used as a carrier. However, only 1.1% of the drug was uptaked by cells at the same time when the drug was charged as a drug solution. Besides, it was also found that the PEGylation of CSO-SA micelles did not affect the intracellular MMC concentrations. This might have resulted from the similar cellular uptake of the micelles and the similar *in vitro* drug release characteristic of MMC-loaded micelles before and after the PEGylation. The above results of the intracellular MMC concentrations corresponded to the results of cytotoxicity for different formulas.

4. Conclusion

The uptake of CSO-SA micelles by macrophage was higher than that by normal liver cells and tumor liver cells. The PEGylation of CSO-SA could significantly reduce the uptake of the micelles by macrophage, but did not affect the cellular uptake by normal liver cells and tumor liver cells. The PEGylation of CSO-SA increased the micelle size and decreased the zeta potential of the micelles, but did not affect the drug entrapment efficiency and *in vitro* drug-release behavior. *In vitro* anti-tumor activity tests indicated that the encapsulation of drug into CSO-SA micelles could increase the cytotoxicity of the drug significantly, and the PEGylation of CSO-SA did not affect the *in vitro* anti-tumor activity of the MMC-loaded micelles. These results indicate that the PEG-CSO-SA micelle is a promising candidate for an intercellular drug delivery carrier.

Acknowledgments

We thank for the financial support of the National Nature Science Foundation of China under Contract Nos. 30472101 and 30672552, and for the financial support of the Zhejiang Provincial Natural Science Foundation under Contract No. z207489.

References

[1] Y. Bae, T.A. Diezi, A. Zhao, G.S. Kwon, Mixed polymeric micelles for combination cancer chemotherapy through the concurrent delivery of multiple chemotherapeutic agents, J. Control. Release 122 (2007) 324–330.
[2] A.I. Minchinton, I.F. Tannock, Drug penetration in solid tumours, Nat. Rev. Cancer 6 (2006) 583–592.
[3] M.R. Kano, Y. Bae, C. Iwata, Y. Morishita, M. Yashiro, M. Oka, T. Fujii, A. Komuro, K. Kiyono, M. Kamiishi, K. Hirakawa, Y. Ouchi, N. Nishiyama, K. Kataoka, K. Miyazono, Improvement of cancer-targeting therapy, using nanocarriers for

intractable solid tumors by inhibition of TGF-beta signaling, Proc. Natl. Acad. Sci. USA 104 (2007) 3460–3465.
[4] R. Duncan, Polymer conjugates as anticancer nanomedicines, Nat. Rev. Cancer 6 (2006) 688–701.
[5] J. Kopecek, P. Kopeckova, T. Minko, Z.R. Lu, HPMA copolymer–anticancer drug conjugates: design, activity, and mechanism of action, Eur. J. Pharm. Biopharm. 50 (2000) 61–81.
[6] N. Nishiyama, K. Kataoka, Current state, achievements, and future prospects of polymeric micelles as nanocarriers for drug and gene delivery, Pharmacol. Ther. 112 (2006) 630–648.
[7] A. Lavasanifar, J. Samue, G.S. Kwon, Poly(ethylene oxide)-block-poly(L-amino acid) micelles for drug delivery, Adv. Drug Deliv. Rev. 54 (2002) 169–190.
[8] K. Kataoka, G.S. Kwon, M. Yokoyama, T. Okano, Y. Sakurai, Block copolymer micelles as vehicles for drug delivery, J. Control. Release 24 (1993) 119–132.
[9] H.M. Aliabadi, D.R. Brocks, L. Afsaneh, Polymeric micelles for the solubilization and delivery of cyclosporine A: pharmacokinetics and biodistribution, Biomaterials 26 (2005) 7251–7259.
[10] G.S. Kwon, Polymeric micelles for delivery of poorly water-soluble compounds, Crit. Rev. Ther. Drug Carrier Syst. 20 (2003) 357–403.
[11] L.B. Li, Y.B. Tan, Preparation and properties of mixed micelles made of pluronic polymer and PEG-PE, J. Colloid Interface Sci. 317 (2008) 326–331.
[12] V. Zabaleta, M.A. Campanero, J.M. Irache, An HPLC with evaporative light scattering detection method for the quantification of PEGs and Gantrez in PEGylated nanoparticles, J. Pharm. Biomed. 44 (2007) 1072–1078.
[13] X. Jiang, H. Dai, K.W. Leong, S.H. Goh, H.Q. Mao, Y.Y. Yang, Chitosan-*g*-PEG/DNA complexes deliver gene to the rat liver via intrabiliary and intraportal infusions, J. Gene Med. 8 (2006) 477–487.
[14] J.Q. Gao, Y. Eto, Y. Yoshioka, F. Sekiguchi, S. Kurachi, T. Morishige, X.L. Yao, H. Watanabe, R. Asavatanabodee, F. Sakurai, H. Mizuguchi, Y. Okada, Y. Mukai, Y. Tsutsumi, T. Mayumi, N. Okada, S. Nakagawa, Effective tumor targeted gene transfer using PEGylated adenovirus vector via systemic administration, J. Control. Release 122 (2007) 102–110.
[15] Y. Tsutsumi, S. Tsunoda, Y. Kaneda, H. Kamada, T. Kihira, S. Nakagawa, Y. Yamamoto, Y. Horisawa, T. Mayumi, In vivo anti-tumor efficacy of polyethylene glycol-modified tumor necrosis factor-alpha against tumor necrosis factor-resistant tumors, Jpn. J. Cancer Res. 87 (1996) 1078–1085.
[16] H. Shibata, Y. Yoshioka, S. Ikemizu, K. Kobayashi, Y. Yamamoto, Y. Mukai, T. Okamoto, M. Taniai, M. Kawamura, Y. Abe, S. Nakagawa, T. Hayakawa, S. Nagata, Y. Yamagata, T. Mayumi, H. Kamada, Y. Tsutsumi, Functionalization of tumor necrosis factor-alpha using phage display technique and PEGylation improves its antitumor therapeutic window, Clin. Cancer Res. 10 (2004) 8293–8300.
[17] Y. Inada, M. Furukawa, H. Sasaki, Y. Kodera, M. Hiroto, H. Nishimura, A. Matsushima, Biomedical and biotechnological applications of PEG- and PM-modified proteins, Trends Biotechnol. 13 (1995) 86–91.
[18] R. Zhou, R. Mazurchuk, R.M. Straubinger, Antivasculature effects of doxorubicin-containing liposomes in an intracranial rat brain tumor model, Cancer Res. 62 (2002) 2561–2566.
[19] T. Terada, M. Mizobata, S. Kawakami, F. Yamashita, M. Hashida, Optimization of tumor-selective targeting by basic fibroblast growth factor-binding peptide grafted PEGylated liposomes, J. Control. Release 119 (2007) 262–270.
[20] H.M. Patel, Serum opsonins and liposomes: their interaction and opsonophagocytosis, Crit. Rev. Ther. Drug Carrier Syst. 9 (1992) 39–90.
[21] J.W. Hong, J.H. Park, K.M. Huh, H. Chung, I.C. Kwon, S.Y. Jeong, PEGylated polyethylenimine for in vivo local gene delivery based on lipiodolized emulsion system, J. Control. Release 99 (2004) 167–176.
[22] Y. Wang, C.Y. Ke, C.W. Beh, S.Q. Liu, S.H. Goh, Y.Y. Yang, The self-assembly of biodegradable cationic polymer micelles as vectors for gene transfection, Biomaterials 28 (2007) 5358–5368.
[23] F.Q. Hu, G.F. Ren, H. Yuan, Y.Z. Du, S. Zeng, Shell cross-linked stearic acid grafted chitosan oligosaccharide self-aggregated micelles for controlled release of paclitaxel, Colloids Surf. B Biointerfaces 50 (2006) 97–103.
[24] F.Q. Hu, M.D. Zhao, H. Yuan, J. You, Y.Z. Du, S. Zeng, A novel chitosan oligosaccharide–stearic acid micelles for gene delivery: properties and in vitro transfection studies, Int. J. Pharm. 315 (2006) 158–166.
[25] J. You, F.Q. Hu, Y.Z. Du, H. Yuan, Polymeric micelles with glycolipid-like structure and multiple hydrophobic domains for mediating-target delivery of paclitaxel, Biomacromolecules 8 (2007) 2450–2456.
[26] J. You, F.Q. Hu, Y.Z. Du, H. Yuan, B.F. Ye, High cytotoxicity and resistant-cell reversal of novel paclitaxel loaded micelles by enhancing molecular-target delivery of the drug, Nanotechnology 18 (2007) 495101.
[27] J.A. Molina-Bolívar, J.M. Hierrezuelo, C. Carnero Ruiz, Self-assembly, hydration, and structures in *N*-decanoyl-*N*-methylglucamide aqueous solutions: effect of salt addition and temperature, J. Colloid Interface Sci. 313 (2007) 656–664.
[28] V.L. Hegde, Y.P. Venkatesh, Generation of antibodies specific to D-mannitol, a unique haptenic allergen, using reductively aminated D-mannose–bovine serum albumin conjugate as the immunogen, Immunobiology 212 (2007) 119–128.
[29] W.J. Li, Z.G. Su, Quantitatively investigating monomethoxypolyethylene glycol modification of protein by capillary electrophoresis, J. Biochem. Biophys. Methods 59 (2004) 65–74.
[30] J. Ahmad, B.T. Ashok, R. Ali, Detection of oxidative DNA damage by a monoclonal antibody: role of lysyl residues in antigen binding, Immunol. Lett. 62 (1998) 87–92.
[31] K.Y. Lee, W.H. Jo, Structural determination and interior polarity of self-aggregates prepared from deoxycholic acid-modified chitosan in water, Macromolecules 31 (1998) 378–383.
[32] T. Mosmann, Rapid colorimetric assay for cellular growth and survival: application to proliferation and cytotoxicity assays, J. Immunol. Methods 65 (1983) 55–63.
[33] H. Eliyahua, A. Joseph, J.P. Schillemans, T. Azzam, A.J. Domb, Y. Barenholz, Characterization and in vivo performance of dextran–sperminepolyplexes and DOTAP/cholesterol lipoplexes administered locally and systemically, Biomaterials 28 (2007) 2339–2349.
[34] E. Bilensoy, O. Ğurkaynak, A. Lale Doğan, A.A. Hıncal, Safety and efficacy of amphiphilic ß-cyclodextrin nanoparticles for paclitaxel delivery, Int. J. Pharm. 347 (2008) 163–170.
[35] I. Montasser, H. Fessi, A.W. Coleman, Atomic force microscopy imaging of novel type of polymeric colloidal nanostructures, Eur. J. Pharm. Biopharm. 54 (2002) 281–284.
[36] W. Chen, H.R. Chen, J.H. Hu, W.L. Yang, C.C. Wang, Synthesis and characterization of polyion complex micelles between poly(ethylene glycol)-grafted poly(aspartic acid) and cetyltrimethyl ammonium bromide, Colloids Surf. A Physicochem. Eng. Aspects 278 (2006) 60–66.
[37] G. Riess, Micellization of block copolymers, Prog. Polym. Sci. 28 (2003) 1107–1170.
[38] S.M. Hussain, K.L. Hess, J.M. Gearhart, K.T. Geiss, J.J. Schlager, In vitro toxicity of nanoparticles in BRL-3A rat liver cells, Toxicol. In Vitro 19 (2005) 975–983.
[39] G. Storm, S.O. Belliot, T. Daemen, D.D. Lasic, Surface modification of nanoparticles to oppose uptake by the mononuclear phagocyte system, Adv. Drug Deliv. Rev. 17 (1995) 31–48.